Cooperative Hoisting with Dual Crawler Cranes under Motion Constraints

Chenhao Cui, Alessandro Giua, Alessandro Pisano

***Abstract*— With the continuous development of industries such as wind power and construction, the weight and complexity of lifted equipment have significantly increased. These lifting tasks often rely on crawler cranes, and the demand for cooperative lifting using dual crawler cranes has grown. However, current operations remain largely manual, leading to safety risks and low efficiency. While extensive research has been conducted on the coordination of overhead cranes and other lifting systems, studies on cooperative control of crawler cranes are still in their early stages and have received insufficient attention. To address this issue, this paper establishes an accurate model of a dual crawler crane system using Lagrange equations. Motion constraints are incorporated to reduce the original fifth-order dynamics to a third-order system, simplifying control implementation. Given the strong coupling characteristics of the underactuated system, a PID-based coupled error compensation control method is proposed to regulate the load's position and attitude precisely. By coordinating cable length adjustments, the proposed method ensures stable and accurate positioning while guaranteeing finite time convergence of cable length errors. Finally, a wind turbine installation scenario is simulated to validate the effectiveness of the proposed control approach.**

I. Introduction

Crawler cranes are widely used in wind power, chemical, and construction industries, often employed for lifting large equipment such as wind turbine blades and distillation towers [1]. With the continuous development of these industries, the weight and shape of the equipment to be lifted are becoming increasingly complex. For tasks requiring high installation precision, such as wind turbine blade or bridge installation, a single crane is inadequate due to its limited capacity and inability to adjust the load's posture, necessitating the collaboration of two cranes [2]. This collaborative operation significantly increases the complexity and safety risks of the lifting process which typically requires multiple experienced operators to work together. During the operation, the lifting path cannot be precisely planned, requiring constant adjustments near the installation position to complete the task. This approach results in significant uncertainty throughout the process and leads to low efficiency.

As a type of mobile crane, a crawler crane can perform pitch and rotational movements when operating independently, lifting loads by adjusting the cable length. However, when two crawler cranes operate collaboratively, safety considerations require the crane bases to remain stable, and the booms are typically fixed. Under these conditions, the lifting and attitude adjustment of the load is achieved solely by controlling the variations in cable length. Therefore, it is essential to suppress load oscillations during the lifting process to enhance safety and efficiency.

Compared to single crane systems, research on dual crane collaborative systems is relatively limited, primarily focusing on modeling, load distribution, and path planning. Research on dual overhead crane systems is conducted in [3]–[5], and different control strategies are proposed to suppress load oscillations. [3] proposes an open loop optimal control strategy for the motion of dual overhead cranes. However, these studies are based on models with fixed cable lengths in dual crane systems, where the cable length is not a system variable, and the load moves only in the horizontal direction. [6]–[9] studies the dual rotary crane system. [6] uses the Lagrange method to establish an accurate model of the dual rotary crane system, but the model still contains dependent variables. [7] proposes a control method that achieves precise control of the load's attitude and position while enhancing the motion synchronization of the two cranes. [8], [9] utilize PID control based on motion constraints for load control, with [9] proposing a scheme that eliminates the need for velocity feedback. Dual rotary cranes adjust the load's position and posture by changing the boom pitch angle, making this operation suitable for lighter loads and lower lifting heights but unsuitable for high-altitude installations such as wind turbine assembly. [10] defines four typical operating modes of dual crawler cranes and employs the PID method for control, ensuring that the object can be hoisted without diagonal pulls on the hoisting ropes. The model in [10], where the hoisting ropes remain vertical without angular deviation, limits the ability to adjust the load's attitude in complex lifting tasks. A method for adjusting the lengths of two cables is proposed to lift the load, treated as a point mass, along a predefined path while satisfying constraints on the cable length velocity [2]. However, in this dual crawler crane system, the load is simply treated as a point mass, which cannot accurately represent the system when lifting long objects such as bridge segments. The dynamic models of the dual overhead crane and dual rotary crane systems are not applicable to the operating mode of the dual crawler crane system. These dual crane systems cannot accomplish tasks requiring significant installation heights, such as the erection of wind turbines [3]–[9]. Moreover, some existing dual crawler crane models simplify the modeling process due to numerous state variables, geometric constraints, and complex coupling relationships. Therefore, a more precise and

Keywords: Cooperative hoisting, Crawler crane, Crane control.

This work was partially supported by project SERICS (PE00000014) under the MUR National Recovery and Resilience Plan funded by the European Union - NextGenerationEU.

The authors are with the Department of Electrical and Electronic Engineering (DIEE), University of Cagliari, Cagliari, Italy, {chenhao.cui, giua, apisano}@unica.it

generalized dynamic model is needed to achieve coordinated control of dual crawler cranes.

To achieve precise control of the load in a dual crawler crane collaborative system, this paper proposes a method that accurately adjusts the load's position and posture while satisfying motion constraints. Specifically, the motion constraints of the system are first defined, followed a fifth order Lagrangian dynamic model was subsequently established for the dual crawler crane system without any linearization assumptions. The non-independent state variables in the model are then eliminated based on the motion constraints, reducing it to a third order system. Additionally, a method is proposed to compute stepwise the non-independent variables present in the model. Finally, a PID-based control method is proposed and applied to a wind turbine installation scenario for simulation-based validation.

The rest of this paper is organized as follows. Section II presents the problem formulation and defines the symbolic variables. Section III establishes the mathematical model of the system. Section IV presents the development process of the controller. Section V validates the effectiveness of the controller through the simulation of a practical case. Section VI concludes the paper and discusses future research directions.

II. Background

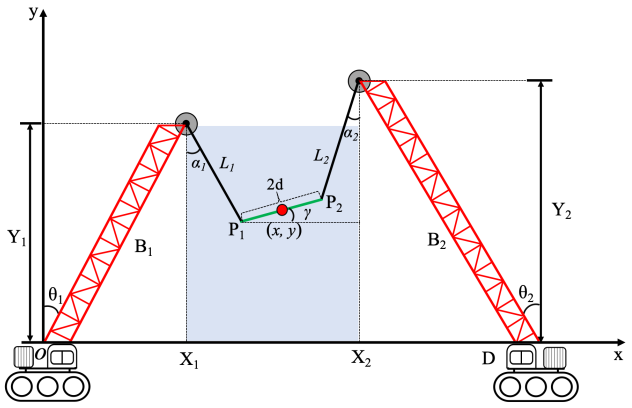

Fig. 1. Schematic representation of two crawler cranes.

A sketch of the two cooperating crawler cranes in the vertical $x-y$ plane is shown in Fig. 1, whose state variables and parameters are defined in Table I. The dual crawler crane system moves the load from an initial to a target position. During this process, the crane bases remain fixed, and the boom pitch angles do not change. Load position and attitude are adjusted solely by varying the lengths of the two cables. In this paper, the cooperative hoisting process involving two cranes is analyzed under the following simplifying assumptions, which are commonly adopted in similar crane related studies:

Assumption 1: In practical applications, the load has a significant mass, ensuring that the cables remain taut at all times while cable elasticity is neglected.

TABLE I
VARIABLES AND PARAMETERS

Symbols	Meanings	Units
$L_1(t), L_2(t)$	rope length	m
$\alpha_1(t), \alpha_2(t)$	cable swing angles	rad
$\gamma(t)$	angle between the load and the horizontal direction	rad
$(x(t), y(t))$	coordinates of the load center	m
θ_1, θ_2	boom pitch angles	rad
B_1, B_2	boom length	m
$2d$	load length	m
D	distance between two cranes	m
$(X_1, Y_1), (X_2, Y_2)$	coordinates of the boom vertex	m
$(x_{p_1}, y_{p_1}), (x_{p_2}, y_{p_2})$	coordinates of P_1, P_2	m
m	payload mass	kg
g	gravity constant	m/s^2

Assumption 2: External disturbances such as winds are neglected in this study but will be considered in future work.

To simplify the description, this paper uses abbreviations as follows:

$$S_\theta = \sin\theta,\ C_\theta = \cos\theta,\ \text{where } \theta \in \begin{cases} \alpha_i, \gamma, \alpha_i \pm \gamma, \alpha_i \pm \alpha_j, \\ i, j = 1, 2,\ (i \neq j). \end{cases}$$

The coordinates of the boom vertices are given by the next straightforward relations (see Fig. 1):

$$\begin{aligned} X_1 &= B_1 \sin\theta_1, \quad Y_1 = B_1 \cos\theta_1, \\ X_2 &= D - B_2 \sin\theta_2, \quad Y_2 = B_2 \cos\theta_2. \end{aligned} \tag{1}$$

The variables $x(t)$, $y(t)$, and $\gamma(t)$ represent the load's position and attitude. Here, $x(t)$ and $y(t)$ denote the coordinates of the payload's center in the X-O-Y coordinate system. Based on geometric relationships, the coordinates of the load center are obtained by solving for the coordinates of its two endpoints P_1 and P_2

$$\begin{aligned} x_{p_1} &= X_1 + L_1 S_{\alpha_1}, \quad y_{p_1} = Y_1 - L_1 C_{\alpha_1}, \\ x_{p_2} &= X_2 - L_2 S_{\alpha_2}, \quad y_{p_2} = Y_2 - L_2 C_{\alpha_2}. \end{aligned} \tag{2}$$

thus

$$\begin{cases} x = \frac{1}{2}(X_1 + X_2 + L_1 S_{\alpha_1} - L_2 S_{\alpha_2}) \\ y = \frac{1}{2}(Y_1 + Y_2 - L_1 C_{\alpha_1} - L_2 C_{\alpha_2}) \end{cases} \tag{3}$$

The admissible load positions within the workspace are determined by the presence of tension in both cables, so that both cranes are carrying part of the load. This region is visually depicted as the shaded area in Fig. 1 and it is analytically described as follows:

$$\begin{cases} \alpha_1, \alpha_2 \in \left(0, \dfrac{\pi}{2}\right),\ \gamma \in \left(-\dfrac{\pi}{2}, \dfrac{\pi}{2}\right), \\ X_1 < x_{p_1} < x < x_{p_2} < X_2, \\ 0 \leq \min(y_{p_1}, y_{p_2}) \leq y \leq \max(y_{p_1}, y_{p_2}) < \min(Y_1, Y_2). \end{cases}$$

III. Mathematical Model

By referring to the schematic in Fig. 1, two constraint equations can be straightforwardly derived as follows by imposing continuity in the horizontal and vertical directions

$$X_1 - X_2 + L_1 S_{\alpha_1} + L_2 S_{\alpha_2} + 2dC_\gamma = 0, \tag{4a}$$
$$Y_1 - Y_2 - L_1 C_{\alpha_1} + L_2 C_{\alpha_2} + 2dS_\gamma = 0. \tag{4b}$$

It is evident that the system has five state variables: $L_1(t), L_2(t), \gamma(t), \alpha_1(t), \alpha_2(t)$. However, the presence of the two constraints (4a)-(4b) indicates that not all five variables are independent, with two of them being determined by the remaining three. Since the dual crane system lifts the load by controlling the lengths $L_1(t)$ and $L_2(t)$, and $\gamma(t)$ represents the load's attitude, we define $L_1(t), L_2(t), \gamma(t)$ as independent variables, whereas $\alpha_1(t)$ and $\alpha_2(t)$ are treated as dependent variables.

The Lagrange method is used to model the dual crawler crane system. To obtain a third order dynamic system with only independent variables, we first establish a fifth order dynamic system that includes dependent variables as follows:

$$\frac{d}{dt}\left(\frac{\partial \mathcal{L}}{\partial \dot{q}_\phi}\right) - \frac{\partial \mathcal{L}}{\partial q_\phi} = u_\phi \tag{5}$$

where $q_\phi = \left[L_1(t), L_2(t), \gamma(t), \alpha_1(t), \alpha_2(t)\right]^\top$ denotes the variable vector, $\dot{q}_\phi = \left[\dot{L}_1(t), \dot{L}_2(t), \dot{\gamma}(t), \dot{\alpha}_1(t), \dot{\alpha}_2(t)\right]^\top$ and $u_\phi = \left[\tau_1(t), \tau_2(t), 0, 0, 0\right]^\top$ represent generalized velocity and the generalized force respectively, where $\tau_1(t), \tau_2(t)$ denote the control inputx. The Lagrangian is given by:

$$\mathcal{L} = T(t) - V(t) \tag{6}$$

To derive the Lagrangian dynamic model of the system, we first define its kinetic and potential energy. Since the boom angle remains fixed during operation, the system's energy depends on the load center coordinates (x, y), where

$$V(t) = mgy \tag{7}$$

Since the load undergoes both translational and rotational motion, its kinetic energy comprises both translational and rotational components

$$T(t) = \frac{1}{2}m\left(\dot{x}^2 + \dot{y}^2\right) + \frac{1}{2}I\dot{\gamma}^2 \tag{8}$$

Its rotational motion can be approximated as that of a uniform straight rod rotating about an axis passing through its center and perpendicular to its length. $I = (md^2)/3$ represents the moment of inertia of the load.

Differentiating the load's midpoint coordinates derived from Eq. (3) yields:

$$\begin{cases} \dot{x} = \frac{1}{2}(\dot{L}_1 S_{\alpha_1} + L_1\dot{\alpha}_1 C_{\alpha_1} - \dot{L}_2 S_{\alpha_2} - L_2\dot{\alpha}_2 C_{\alpha_2}) \\ \dot{y} = \frac{1}{2}(L_1\dot{\alpha}_1 S_{\alpha_1} - \dot{L}_1 C_{\alpha_1} + L_2\dot{\alpha}_2 S_{\alpha_2} - \dot{L}_2 C_{\alpha_2}) \end{cases} \tag{9}$$

Substituting Eq. (9) into Eq. (8) one obtains

$$\begin{aligned} T(t) =& \frac{1}{8}m(\dot{L}_1^2 + L_1^2\dot{\alpha}_1^2 + L_2^2\dot{\alpha}_2^2 + 2\dot{L}_1\dot{L}_2 C_{(\alpha_1+\alpha_2)} \\ & - 2\dot{L}_1 L_2\dot{\alpha}_2 S_{(\alpha_1+\alpha_2)} - 2L_1\dot{L}_2\dot{\alpha}_1 S_{(\alpha_1+\alpha_2)} \\ & - 2L_1 L_2\dot{\alpha}_1\dot{\alpha}_2 C_{(\alpha_1+\alpha_2)} + \dot{L}_2^2) + \frac{1}{6}md^2\dot{\gamma}^2 \end{aligned} \tag{10}$$

Similarly, substituting Eq. (3) into Eq. (7) one obtains

$$V(t) = \frac{1}{2}mg(Y_1 + Y_2 - L_1 C_{\alpha_1} - L_2 C_{\alpha_2}) \tag{11}$$

Since the potential energy of the system $V(t)$ does not contain the $\dot{q}_\phi$ term, Eq. (5) can be rewritten as

$$\frac{d}{dt}\left(\frac{\partial T}{\partial \dot{q}_\phi}\right) - \frac{\partial T}{\partial q_\phi} + \frac{\partial V}{\partial q_\phi} = u_\phi \tag{12}$$

Then, the dynamic equations of the system can be defined as the following forms

$$\begin{cases} \mathcal{F}_{L_i} \overset{\text{def}}{=} \frac{d}{dt}\left(\frac{\partial T}{\partial \dot{L}_i}\right) - \frac{\partial T}{\partial L_i} + \frac{\partial V}{\partial L_i} = \tau_i(t) \\ \mathcal{F}_\gamma \overset{\text{def}}{=} \frac{d}{dt}\left(\frac{\partial T}{\partial \dot{\gamma}}\right) - \frac{\partial T}{\partial \gamma} + \frac{\partial V}{\partial \gamma} \\ \mathcal{F}_{\alpha_i} \overset{\text{def}}{=} \frac{d}{dt}\left(\frac{\partial T}{\partial \dot{\alpha}_i}\right) - \frac{\partial T}{\partial \alpha_i} + \frac{\partial V}{\partial \alpha_i},\ i = 1, 2 \end{cases} \tag{13}$$

where the accurate expression are expressed as follows

$$\begin{aligned} \mathcal{F}_{L_1} =& \frac{1}{4}m\big(\ddot{L}_1 - L_1\dot{\alpha}_1^2 - (2\dot{L}_2\dot{\alpha}_2 + L_2\ddot{\alpha}_2)S_{(\alpha_1+\alpha_2)} \\ & + (\ddot{L}_2 - L_2\dot{\alpha}_2^2)C_{(\alpha_1+\alpha_2)} - 2gC_{\alpha_1}\big), \\ \mathcal{F}_{L_2} =& \frac{1}{4}m\big(\ddot{L}_2 - L_2\dot{\alpha}_2^2 - (2\dot{L}_1\dot{\alpha}_1 + L_1\ddot{\alpha}_1)S_{(\alpha_1+\alpha_2)} \\ & + (\ddot{L}_1 - L_1\dot{\alpha}_1^2)C_{(\alpha_1+\alpha_2)} - 2gC_{\alpha_2}\big), \\ \mathcal{F}_\gamma =& \frac{1}{3}md^2\ddot{\gamma}, \\ \mathcal{F}_{\alpha_1} =& \frac{1}{4}m\big(2L_1\dot{L}_1\dot{\alpha}_1 + L_1^2\ddot{\alpha}_1 + 2gL_1 S_{\alpha_1} \\ & - (2L_1\dot{L}_2\dot{\alpha}_2 + L_1 L_2\ddot{\alpha}_2)C_{(\alpha_1+\alpha_2)} \\ & + (L_1 L_2\dot{\alpha}_2^2 - L_1\ddot{L}_2)S_{(\alpha_1+\alpha_2)}\big), \\ \mathcal{F}_{\alpha_2} =& \frac{1}{4}m\big(2L_2\dot{L}_2\dot{\alpha}_2 + L_2^2\ddot{\alpha}_2 + 2gL_2 S_{\alpha_2} \\ & - (2\dot{L}_1 L_2\dot{\alpha}_1 + L_1 L_2\ddot{\alpha}_1)C_{(\alpha_1+\alpha_2)} \\ & + (L_1 L_2\dot{\alpha}_1^2 - \ddot{L}_1 L_2)S_{(\alpha_1+\alpha_2)}\big). \end{aligned} \tag{14}$$

To simplify the description and facilitate the subsequent analysis, we derive the dynamic equation with five state variables, including α_1 and α_2, based on Eq. (14). It is expressed in the following compact matrix-vector form:

$$M'(q_\phi)\ddot{q}_\phi + C'(q_\phi, \dot{q}_\phi)\dot{q}_\phi + G'(q_\phi) = u_\phi \tag{15}$$

where $M'(q_\phi), C'(q_\phi, \dot{q}_\phi) \in \mathbb{R}^{5\times5}$, $G'(q_\phi) \in \mathbb{R}^5$ are the inertia matrix, centripetal Coriolis matrix and gravity vector respectively. After arrangement, the matrices in Eq. (15) are expressed as follows

$$M'(q_\phi) = \begin{bmatrix} \frac{1}{4}m & M'_{12} & 0 & 0 & M'_{15} \\ M'_{12} & \frac{1}{4}m & 0 & M'_{24} & 0 \\ 0 & 0 & \frac{1}{3}md^2 & 0 & 0 \\ 0 & M'_{24} & 0 & \frac{1}{4}mL_1^2 & M'_{45} \\ M'_{15} & 0 & 0 & M'_{45} & \frac{1}{4}mL_2^2 \end{bmatrix},$$

$$C'(q_\phi, \dot{q}_\phi) = \begin{bmatrix} 0 & C'_{12} & 0 & C'_{14} & C'_{15} \\ C'_{21} & 0 & 0 & C'_{24} & C'_{25} \\ 0 & 0 & 0 & 0 & 0 \\ C'_{41} & C'_{42} & 0 & 0 & C'_{45} \\ C'_{51} & C'_{52} & 0 & C'_{54} & 0 \end{bmatrix} G'(q_\phi) = \begin{bmatrix} -\frac{1}{2}mgC_{\alpha_1} \\ -\frac{1}{2}mgC_{\alpha_2} \\ 0 \\ \frac{1}{2}mgL_1 S_{\alpha_1} \\ \frac{1}{2}mgL_2 S_{\alpha_2} \end{bmatrix}. \tag{16}$$

where the detailed expressions of the elements of $M'(q_\phi)$ and $C'(q_\phi, \dot{q}_\phi)$ are provided in the Appendix. However, the five state variables system includes the dependent variables α_1 and α_2, and the dynamic model does not account for the constraints (4a)-(4b). The next step is to incorporate these constraints into the model and transform it into a three-state variables system. $\alpha_1(t)$ and $\alpha_2(t)$ can in fact be regarded as dependent variables of $L_1(t), L_2(t)$ and $\gamma(t)$ and redefined as follows according to (4a)-(4b)

$$\alpha_1 = h(L_1, L_2, \gamma), \tag{17}$$

$$\alpha_2 = k(L_1, L_2, \gamma). \tag{18}$$

Although an explicit representation of functions h and k appears to be not possible to derive by Eqs. (4a)-(4b), some useful manipulations are presented next. Taking the temporal derivative of (17) and (18) one obtains

$$\begin{aligned} \dot{\alpha}_1 &= \frac{\partial h}{\partial L_1}\dot{L}_1 + \frac{\partial h}{\partial L_2}\dot{L}_2 + \frac{\partial h}{\partial \gamma}\dot{\gamma}, \\ \dot{\alpha}_2 &= \frac{\partial k}{\partial L_1}\dot{L}_1 + \frac{\partial k}{\partial L_2}\dot{L}_2 + \frac{\partial k}{\partial \gamma}\dot{\gamma}. \end{aligned} \tag{19}$$

Eq. (19) can be rewritten in the more compact form as follows:

$$\begin{aligned} \dot{\alpha_1} &= h_{L_1}\dot{L}_1 + h_{L_2}\dot{L}_2 + h_\gamma\dot{\gamma}, \\ \dot{\alpha_2} &= k_{L_1}\dot{L}_1 + k_{L_2}\dot{L}_2 + k_\gamma\dot{\gamma}. \end{aligned} \tag{20}$$

To derive the expressions for the coefficients h_{L_1}, h_{L_2},...,k_γ in Eq. (20), take the partial derivative of constraints Eq. (4a) and Eq. (4b) with respect to L_1, yielding:

$$\begin{aligned} S_{\alpha_1} + L_1 h_{L_1} C_{\alpha_1} + L_2 k_{L_1} C_{\alpha_2} = 0, \\ L_1 h_{L_1} S_{\alpha_1} - C_{\alpha_1} - L_2 k_{L_1} S_{\alpha_2} = 0. \end{aligned} \tag{21}$$

The expressions for h_{L_1} and k_{L_1} can then be computed as follows

$$h_{L_1} = \frac{C_{(\alpha_1+\alpha_2)}}{L_1 S_{(\alpha_1+\alpha_2)}}, \quad k_{L_1} = -\frac{1}{L_2 S_{(\alpha_1+\alpha_2)}}. \tag{22}$$

Similarly, take the partial derivative of constraints Eq. (4a) and Eq. (4b) with respect to L_2 and γ. Straightforward manipulations yield

$$\begin{aligned} h_{L_2} &= -\frac{1}{L_1 S_{(\alpha_1+\alpha_2)}}, \quad k_{L_2} = \frac{C_{(\alpha_1+\alpha_2)}}{L_2 S_{(\alpha_1+\alpha_2)}}, \\ h_\gamma &= -\frac{2dC_{(\alpha_2+\gamma)}}{L_1 S_{(\alpha_1+\alpha_2)}}, \quad k_\gamma = \frac{2dC_{(\alpha_1-\gamma)}}{L_2 S_{(\alpha_1+\alpha_2)}}. \end{aligned} \tag{23}$$

At this stage, we derive the dynamic equations for the three state variables system using the Lagrange equation (12)

$$\frac{d}{dt}\left(\frac{\partial T}{\partial \dot{q}}\right) - \frac{\partial T}{\partial q} + \frac{\partial V}{\partial q} = u \tag{24}$$

where $q = \left[L_1(t), L_2(t), \gamma(t)\right]^\top$ represent the vector of generalized Lagrangian coordinates, and $u = \left[\tau_1(t), \tau_2(t), 0\right]^\top$ denotes the generalized force vector. After arrangement, the constrained three state variables dynamic model can be defined in the following form based on Eqs.(14) and (22-24):

$$\begin{cases} \mathcal{F}_{L_1} + h_{L_1}\mathcal{F}_{\alpha_1} + k_{L_1}\mathcal{F}_{\alpha_2} = \tau_1(t) \\ \mathcal{F}_{L_2} + h_{L_2}\mathcal{F}_{\alpha_1} + k_{L_2}\mathcal{F}_{\alpha_2} = \tau_2(t) \\ \mathcal{F}_\gamma + h_\gamma\mathcal{F}_{\alpha_1} + k_\gamma\mathcal{F}_{\alpha_2} = 0 \end{cases} \tag{25}$$

Similarly, Eq. (25) can be rewritten in the following form:

$$M(q_\phi)\ddot{q} + C(q_\phi, \dot{q}_\phi)\dot{q} + G(q_\phi) = u \tag{26}$$

where $M(q_\phi), C(q_\phi, \dot{q}_\phi) \in \mathbb{R}^{3\times3}$, $G(q) \in \mathbb{R}^3$ are the inertia matrix, centripetal Coriolis matrix and gravity vector respectively. According to (20), we can obtain the relationship between $\dot{q}$ and $\dot{q}_\phi$ as follows

$$\dot{q}_\phi = N\dot{q}, \quad u = N^\top u_\phi. \tag{27}$$

where

$$N^\top = \begin{bmatrix} 1 & 0 & 0 & h_{L_1} & k_{L_1} \\ 0 & 1 & 0 & h_{L_2} & k_{L_2} \\ 0 & 0 & 1 & h_\gamma & k_\gamma \end{bmatrix} \tag{28}$$

Differentiating both sides of Eq. (27) yields:

$$\ddot{q}_\phi = \dot{N}\dot{q} + N\ddot{q} \tag{29}$$

Substituting Eq. (27) and Eq. (29) into Eq. (15) one obtains

$$(N^\top M' N)\ddot{q} + N^\top(M'\dot{N} + C'N)\dot{q} + N^\top G' = N^\top u_\phi \tag{30}$$

Defining

$$\begin{aligned} &M(q_\phi) = N^\top M'(q_\phi)N,\ G(q_\phi) = N^\top G'(q_\phi),\ u = N^\top u_\phi, \\ &C(q_\phi, \dot{q}_\phi) = N^\top M'(q_\phi)\dot{N} + N^\top C'(q_\phi, \dot{q}_\phi)N \end{aligned} \tag{31}$$

the dynamic model is finally presented as follows:

$$M(q_\phi)\ddot{q} + C(q_\phi, \dot{q}_\phi)\dot{q} + G(q_\phi) = u - F\dot{q} \tag{32}$$

where $F \in \mathbb{R}^{3\times3}$ is a diagonal matrix containing the friction coefficients. Through subsequent computations and arrangements, $G(q_\phi)$ is derived as follows

$$G = \begin{bmatrix} \frac{1}{2}h_{L_1}mgL_1S_{\alpha_1} + \frac{1}{2}k_{L_1}mgL_2S_{\alpha_2} - \frac{1}{2}mgC_{\alpha_1} \\ \frac{1}{2}h_{L_2}mgL_1S_{\alpha_1} + \frac{1}{2}k_{L_2}mgL_2S_{\alpha_2} - \frac{1}{2}mgC_{\alpha_2} \\ \frac{1}{2}h_\gamma mgL_1S_{\alpha_1} + \frac{1}{2}k_\gamma mgL_2S_{\alpha_2} \end{bmatrix} \tag{33}$$

and the detailed expressions of the elements of matrices $M(q_\phi)$ and $C(q_\phi, \dot{q}_\phi)$ are provided in the Appendix.

IV. Controller development

A. Control Objectives

In the practical scenarios, the load must be lifted from a known initial position to a specified installation position. The dual crawler crane system adjusts the load's attitude and position by controlling the lengths of two cables. This paper aims to design a controller to enhance positioning accuracy and suppress load oscillations. Let $L_{1d}(t)$, $L_{2d}(t)$ and $\gamma_d(t)$ denote the desired profiles. Our goal is to ensure that the cable lengths $L_1(t)$ and $L_2(t)$, as well as the payload swing $\gamma(t)$ to asymptotically converge to the desired profiles within a small vicinity as

$$\lim_{t\to\infty} L_1(t) = L_{1d}(t), \lim_{t\to\infty} L_2(t) = L_{2d}(t),$$

$$\lim_{t\to\infty} \gamma(t) = \gamma_d(t).$$

B. Controller design

The dual crawler crane system is an underactuated system, where the number of control variables exceeds the available control inputs. Non-actuated variables can only be controlled

indirectly based on complex coupling dynamics, increasing the difficulty of the control problem. To address this challenge, a coupled error compensation control strategy is proposed. Inspired by [11], [12], the following control error signals are designed:

$$\begin{aligned} e_1(t) &= \dot{L}_{1d} - \dot{L}_1 + \eta_{11}(L_{1d} - L_1) - \eta_{12}(\gamma - \gamma_d), \\ e_2(t) &= \dot{L}_{2d} - \dot{L}_2 + \eta_{21}(L_{2d} - L_2) + \eta_{22}(\gamma - \gamma_d). \end{aligned} \tag{34}$$

where η_{ij} $(i, j = 1, 2)$ are positive gains. These error signals incorporate position and velocity errors while introducing a swing-dependent compensation term devoted to provide active swing damping during the load travel once the error signals $e_1(t)$ and $e_2(t)$ are steered in a vicinity of zero. The formal proof that the vanishing of $e_1(t)$ and $e_2(t)$ ensures the attainment of the control objective goes beyond the scope of this paper and will be presented in next works by suitably generalizing the analysis presented in [11] to the more complicated dual crane system dynamics under investigation. PID-based control inputs τ_i (i=1,2) of the form $\tau_i = PID(e_i)$, with gains K_{pi}, K_{ii} and K_{di} are considered.

C. Numerical solution of (31)-(33)

Note that in system (31)-(33), the state vector q comprises only the independent variables L_1, L_2, and γ, whereas the elements of matrices M, C and G are also affected by the dependent variables α_1 and α_2. To address this issue, a stepwise numerical solution method is proposed.

System (31)-(33) is solved numerically in order to get q_k and $\dot{q}_k$, for $k = 0, 1, 2, \ldots, N$ with $t_0 = 0, t_N = T$. Here, N is the total number of time steps in the interval $[t_0, t_N] = [0, T]$. Definition of q_k is $q_k = q(t_k)$, similarly for other terms. At each time step t_k, α_{1k} and α_{2k} are computed by solving numerically the constraint equations (4a, 4b) using the current values of $q_k = [L_{1k}, L_{2k}, \gamma_k]$. This procedure is outlined in the next algorithm.

Algorithm 1 Stepwise Numerical Computation of α_1, α_2

Input: Initial state variables: L_{10}, L_{20}, γ_0

for *each time step* $t_k, k = 0, 1, 2, \ldots, N$ **do**

Compute α_{1k}, α_{2k} by solving the constraint equations (4a, 4b).

Compute the next values of $L_{1k+1}, L_{2k+1}, \gamma_{k+1}$ by solving the system dynamics (31)-(33).

V. Simulation Case Study

Fig. 2 illustrates the installation of a 125 kW wind turbine, focusing on the hoisting process of a single turbine blade. The blade has a length of 20 m and a weight of 1,800 kg, and it must be installed at a height of 50 m while maintaining a 42° angle relative to the horizontal. For this typical task, the general operating parameters of the crawler cranes are listed in Table II.

Based on the initial and installation positions of the wind turbine blade, the initial values of L_1, L_2 and γ and the final target values are determined as follows:

$$L_{10} = 90.55 \text{ m}, \ L_{20} = 100.5 \text{ m}, \ \gamma_0 = 0 \text{ rad},$$
$$L_{1f} = 49.55 \text{ m}, \ L_{2f} = 44.46 \text{ m}, \ \gamma_f = 0.73 \text{ rad}.$$

The desired L_1, L_2 and γ profiles are all chosen so as to enforce a constant-velocity transition from the initial values at $t_0 = 0$s to the target values at $t_f = 15$s (the corresponding plots of $L_{1d}(t), L_{2d}(t)$ and $\gamma_d(t)$ are displayed in Fig. 3). Also set the system evolution time $T = 20$s. After trial-and-error tuning, the gain parameters are set as follows

$$\eta_{11} = \eta_{21} = 20, \ \eta_{12} = \eta_{22} = 550, \ K_{p1} = K_{p2} = 100,$$
$$K_{i1} = K_{i2} = 0.8, \ K_{d1} = K_{d2} = 3.$$

The simulation of the case study was conducted using MATLAB, and the results are presented in Fig. 3.

As shown in Fig. 3, the actual cable lengths closely

Fig. 2. Cooperative hoisting of wind turbines with two crawler cranes.

TABLE II
Parameter Values

Symbols	Values	Symbols	Values
θ_1	0.22 rad	θ_2	0.2 rad
B_1	92 m	B_2	102 m
$2d$	20 m	D	80 m
m	1800 kg	g	9.81 m/s^2
F	diag(0.5, 0.5, 0.4)		

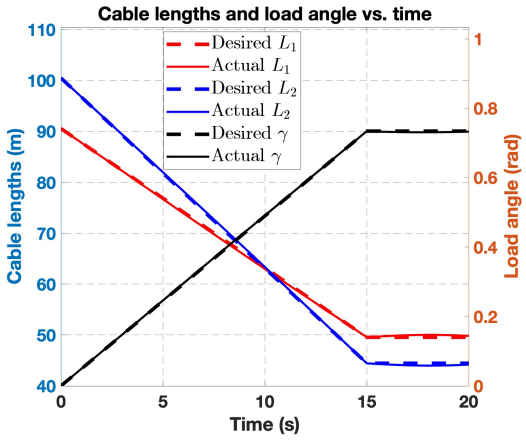

Fig. 3. Rope lengths L_1, L_2 and load angle γ over time.

follow the desired profiles, indicating that the control strategy effectively regulates L_1 and L_2. The transition between different phases occurs smoothly, with minimal steady state error. The payload swing angle γ increases steadily and converges to the expected value. The system maintains stability throughout the process, demonstrating the controller's ability to manage coupled dynamics while ensuring accurate trajectory tracking. The simulation results confirm that the proposed control approach achieves precise length regulation and swing angle convergence, effectively guiding the payload to its target position.

VI. Conclusion

This paper investigates the cooperative lifting problem of two tracked cranes under motion constraints. A PID-based coupled error compensation control method is proposed to regulate the load position and orientation, ensuring precise trajectory tracking. Simulation results demonstrate that the proposed method allows the load to accurately follow the predefined trajectory while effectively reducing load swing during lifting. In future work, the influences of real world disturbances such as strong winds, as well as cable elasticity during lifting, will be considered to establish a more accurate and realistic model and further reduce load swing during operation.

Appendix

$$
\begin{aligned}
&M'_{12} = mC_{(\alpha_1+\alpha_2)}/4, \quad M'_{15} = -mL_2S_{(\alpha_1+\alpha_2)}/4,\\
&M'_{24} = -mL_1S_{(\alpha_1+\alpha_2)}/4, \quad M'_{45} = -mL_1L_2C_{(\alpha_1+\alpha_2)}/4,\\
&C'_{12} = -m\dot{\alpha}_2S_{(\alpha_1+\alpha_2)}/2, \quad C'_{14} = -mL_1\dot{\alpha}_1/4,\\
&C'_{15} = -mL_2\dot{\alpha}_2C_{(\alpha_1+\alpha_2)}/4, \; C'_{21} = -m\dot{\alpha}_1S_{(\alpha_1+\alpha_2)}/2,\\
&C'_{24} = -mL_1\dot{\alpha}_1C_{(\alpha_1+\alpha_2)}/4, \quad C'_{25} = -mL_2\dot{\alpha}_2/4,\\
&C'_{41} = mL_1\dot{\alpha}_1/2, \quad C'_{42} = -mL_1\dot{\alpha}_2C_{(\alpha_1+\alpha_2)}/2,\\
&C'_{45} = mL_1L_2\dot{\alpha}_2S_{(\alpha_1+\alpha_2)}/4, \quad C'_{52} = mL_2\dot{\alpha}_2/2,\\
&C'_{51} = -mL_2\dot{\alpha}_1C_{(\alpha_1+\alpha_2)}/2, \; C'_{54} = mL_1L_2\dot{\alpha}_1S_{(\alpha_1+\alpha_2)}/4,\\
&M_{11} = m(L_1^2h_{L_1}^2 + L_2^2k_{L_1}^2 - 2C_{(\alpha_1+\alpha_2)}L_1L_2h_{L_1}k_{L_1}\\
&\quad - 2S_{(\alpha_1+\alpha_2)}L_2k_{L_1} + 1)/4,\\
&M_{12} = M_{21} = m(h_{L_1}h_{L_2}L_1^2 + k_{L_1}k_{L_2}L_2^2\\
&\quad + (1 - h_{L_1}k_{L_2} - h_{L_2}k_{L_1})L_1L_2C_{(\alpha_1+\alpha_2)}\\
&\quad - (h_{L_1}L_1 + k_{L_2}L_2)S_{(\alpha_1+\alpha_2)})/4,\\
&M_{13} = M_{31} = m(h_{L_1}h_\gamma L_1^2 + k_{L_1}k_\gamma L_2^2\\
&\quad - (h_{L_1}k_\gamma + h_\gamma k_{L_1})L_1L_2C_{(\alpha_1+\alpha_2)} - k_\gamma L_2S_{(\alpha_1+\alpha_2)})/4,\\
&M_{22} = m({L_1}^2h_{L_2}^2 + L_2^2k_{L_2}^2 - 2C_{(\alpha_1+\alpha_2)}L_1L_2h_{L_2}k_{L_2}\\
&\quad - 2S_{(\alpha_1+\alpha_2)}L_1h_{L_2} + 1)/4,\\
&M_{23} = M_{32} = m(h_{L_2}h_\gamma L_1^2 + k_{L_2}k_\gamma L_2^2\\
&\quad - (h_{L_2}k_\gamma + h_\gamma k_{L_2})L_1L_2C_{(\alpha_1+\alpha_2)} - h_\gamma L_1S_{(\alpha_1+\alpha_2)})/4,\\
&M_{33} = m(3L_1^2h_\gamma^2 + 3L_2^2k_\gamma^2 + 4d^2 - 6L_1L_2h_\gamma k_\gamma C_{(\alpha_1+\alpha_2)})/12,
\end{aligned}
$$

$$
\begin{aligned}
&C_{11} = m(\dot{\alpha}_1L_1h_{L_1} - (2\dot{\alpha}_1 + \dot{\alpha}_2)L_2k_{L_1}C_{(\alpha_1+\alpha_2)}\\
&\quad + (L_1\dot{\alpha}_1 + \dot{\alpha}_2)L_2h_{L_1}k_{L_1}S_{(\alpha_1+\alpha_2)})/4,\\
&C_{12} = m(2L_2k_{L_1}\dot{\alpha}_2 - (L_1h_{L_1} + L_2k_{L_2})C_{(\alpha_1+\alpha_2)}\dot{\alpha}_2\\
&\quad + (L_1L_2h_{L_1}k_{L_2}\dot{\alpha}_2 + L_1L_2h_{L_2}k_{L_1}\dot{\alpha}_1 - 2)S_{(\alpha_1+\alpha_2)}\\
&\quad - L_1h_{L_1}\dot{\alpha}_1)/4,\\
&C_{13} = m(L_1L_2S_{(\alpha_1+\alpha_2)}(h_{L_1}k_\gamma\dot{\alpha}_2 + h_\gamma k_{L_1}\dot{\alpha}_1)\\
&\quad - L_2k_\gamma C_{(\alpha_1+\alpha_2)}\dot{\alpha}_2 - L_1h_\gamma\dot{\alpha}_1)/4,\\
&C_{21} = m(2L_1h_{L_2}\dot{\alpha}_1 - (L_1h_{L_1} + 2L_2k_{L_2})C_{(\alpha_1+\alpha_2)}\dot{\alpha}_1\\
&\quad + L_1L_2S_{(\alpha_1+\alpha_2)}(h_{L_1}k_{L_2}\dot{\alpha}_1 + h_{L_2}k_{L_1}\dot{\alpha}_2)\\
&\quad - 2S_{(\alpha_1+\alpha_2)}\dot{\alpha}_1 - L_2k_{L_1}\dot{\alpha}_2)/4,\\
&C_{22} = m(L_2k_{L_2}\dot{\alpha}_2 - L_1h_{L_2}C_{(\alpha_1+\alpha_2)}(\dot{\alpha}_1 + 2\dot{\alpha}_2)\\
&\quad + L_1L_2h_{L_2}k_{L_2}S_{(\alpha_1+\alpha_2)}(\dot{\alpha}_1 + \dot{\alpha}_2))/4,\\
&C_{23} = m((h_{L_2}k_\gamma\dot{\alpha}_2 + h_\gamma k_{L_2}\dot{\alpha}_1)L_1L_2S_{(\alpha_1+\alpha_2)}\\
&\quad - L_1h_\gamma C_{(\alpha_1+\alpha_2)}\dot{\alpha}_1 - L_2k_\gamma\dot{\alpha}_2)/4,\\
&C_{31} = m((h_{L_1}k_\gamma\dot{\alpha}_1 + h_\gamma k_{L_1}\dot{\alpha}_2)L_1L_2S_{(\alpha_1+\alpha_2)}\\
&\quad + 2L_1h_\gamma\dot{\alpha}_1 - 2L_2k_\gamma\dot{\alpha}_1C_{(\alpha_1+\alpha_2)})/4,\\
&C_{32} = m((h_{L_2}k_\gamma\dot{\alpha}_1 + h_\gamma k_{L_2}\dot{\alpha}_2)L_1L_2S_{(\alpha_1+\alpha_2)}\\
&\quad + 2L_2k_\gamma\dot{\alpha}_2 - 2L_1h_\gamma\dot{\alpha}_2C_{(\alpha_1+\alpha_2)})/4,\\
&C_{33} = m(\dot{\alpha}_1 + \dot{\alpha}_2)L_1L_2h_\gamma k_\gamma S_{(\alpha_1+\alpha_2)}/4.
\end{aligned}
$$

References

[1] X. Shen, J. An, and T. Terano, "Calculation method of load distribution for two-crane cooperative lift," in *2018 37th Chinese Control Conference (CCC)*, 2018, pp. 7851–7855.

[2] C. Cui, A. Giua, and A. Pisano, "Cooperative hoisting with two crawler cranes under rope-velocity constraints," in *2023 IEEE Conference on Control Technology and Applications (CCTA)*, 2023, pp. 978–983.

[3] A. V. Perig, A. N. Stadnik, A. A. Kostikov, and S. V. Podlesny, "Research into 2d dynamics and control of small oscillations of a cross-beam during transportation by two overhead cranes," *Shock and Vibration*, vol. 2017, no. 1, p. 9605657, 2017.

[4] S. Raj and B. S. Reddy, "Anti-swing control in an underactuated dual overhead crane," in *2023 23rd International Conference on Control, Automation and Systems (ICCAS)*, 2023, pp. 426–431.

[5] B. Lu, Y. Fang, and N. Sun, "Modeling and nonlinear coordination control for an underactuated dual overhead crane system," *Automatica*, vol. 91, pp. 244–255, 2018.

[6] Y. Fu, T. Yang, N. Sun, J. Zhang, and Y. Fang, "Dynamics modeling and analysis for cooperative dual rotary crane systems," in *2018 37th Chinese Control Conference (CCC)*, 2018, pp. 5492–5497.

[7] Z. Liu, N. Sun, T. Yang, G. Liu, and Y. Fang, "Assembly-oriented finite-time coordinated control of underactuated dual rotary cranes for payload position and attitude regulation," *IEEE Transactions on Automation Science and Engineering*, vol. 21, no. 3, pp. 3678–3690, 2024.

[8] Z. Liu, Y. Fu, N. Sun, T. Yang, and Y. Fang, "Collaborative antiswing hoisting control for dual rotary cranes with motion constraints," *IEEE Transactions on Industrial Informatics*, vol. 18, no. 9, pp. 6120–6130, 2022.

[9] N. Sun, Y. Fu, T. Yang, J. Zhang, Y. Fang, and X. Xin, "Nonlinear motion control of complicated dual rotary crane systems without velocity feedback: Design, analysis, and hardware experiments," *IEEE Transactions on Automation Science and Engineering*, vol. 17, no. 2, pp. 1017–1029, 2020.

[10] Y. Li, X. Xi, J. Xie, and C. Liu, "Study and implementation of a cooperative hoisting for two crawler cranes," *Journal of Intelligent & Robotic Systems*, vol. 83, pp. 165–178, 2016.

[11] G. Bartolini, A. Pisano, and E. Usai, "Second-order sliding-mode control of container cranes," *Automatica*, vol. 38, no. 10, pp. 1783–1790, 2002.

[12] ——, "Output-feedback control of container cranes: a comparative analysis," in *Proceedings of the 41st IEEE Conference on Decision and Control, 2002.*, vol. 3, 2002, pp. 3237–3242 vol.3.